Interfaces of Ionic Liquids

Milton Ponte
miltonponte@tecnico.ulisboa.pt

Instituto Superior Técnico, Lisboa, Portugal

October 2021

Abstract

This work focused on understanding the structure and behavior of $[C_{18}mim]^+[Cl]^-$ at the interface of pure and salted water. It consisted of molecular dynamics simulations of the system, employing an all-atom force field, at different areas per molecule, both in pure water and in water with 0.5 M of $NaCl$. The study focused on visual, density profile, and alkyl chain organization analysis.

The results showed that, in pure water, the cations aggregate at the surface even at high areas per molecule (9.2 nm^2/molecule) and present a structure very compact, with an high degree of organization and with closer cations organizing in an anti-parallel arrangement, which is promoted by the high degree of dissolution of the chloride anions. For more compacted systems, at lower areas per molecule, the cations form hemispherical cylinders at the surface of water, which eventually collapse into micelles upon compression, with an average aggregation number of 122.

In water with 0.5 M of $NaCl$, the cations present a very similar structure. With relation to the results in pure water, in salted water the simulations predict the anions to be closer to the cations' rings. The hemispherical cylinders observed at 0.36 nm^2/molecule are smaller and more organized. Micelle formation was still observed.

Keywords: 1-alkyl-3-imidazolium, Ionic Liquids, C18mim, [C18mim][Cl], Molecular Dynamics, Amphiphilic Molecules, Air-Water Interface

1. Introduction

Ionic Liquids (IL) are molten salts composed solely on ions, without the presence of solvent, which have a melting temperature below 100℃. These Ionic Liquids are divided in subclasses, based on melting temperature and other properties. One example could be Room Temperature Ionic Liquids (RTIL), which represents ILs with melting temperatures below 25℃.

These liquids gained significant relevance on the premise of being environmentally friendly due to their negligible vapor pressure at ambient conditions, with many of the compounds not presenting signs of distillation below decomposition temperatures [1]. They are used for a wide array of applications, which include electrochemistry, alkylation, capture of toxic substances, hydrogenation, performance additives, ect. [2].

Many possible applications of ILs depend on the knowledge available regarding their interfacial properties, which has been poorly investigated in the past.

The wide range of properties, especially amphiphilicity, and its effect on structure, leads to the possibility of ILs behaving like ionic surfactants, forming structures such as micelles, or forming Gibbs and Langmuir Films at the air-water interface.

Gibbs films occur when the molecules tend to be more hydrophilic, which leads to some of them dissolving in the water. The film is for the most part in a condense state at low temperature [3]. These films follow equations of state that can be deducted from the Gibbs Adsorption Isotherm.

Langmuir Films are insoluble molecular films deposited on the surface of a liquid and are commonly formed by amphiphilic molecules that tend to be more hydrophobic and self-assemble into two-dimensional systems at the air-water interface [4].

These films are of particular interest because of their possible applications, such as modeling of systems for membrane biophysics; modeling of chemical, photochemical and biochemical surface reactions; and fabrication of Langmuir-Blodgett Films.

Several studies have been done, with special focus on 1-alkyl-3-methylimidazolium systems with the $[NTf2]^-$ anion. These systems present high hydrophobicity of both the $[NTf2]^-$ anion and the longer alkyl chains, thus favoring the formation of Langmuir Films at the surface of the water.

In 2016, Filipe *et al* reported the formation

of Langmuir Films of $[C_{18}mim]^+[NTf2]^-$ at the air-water interface displaying crystalline-like structures, with the experimental results being validated with the aid of MD simulations [5].

Colaço simulated the system of $[C_{20}mim]^+[NTf2]^-$ at the air-water interface, recurring to Molecular Dynamics. She observed that the system can display a mono or trilayer structure, depending on the surface area of the interface, in agreement with the observations that had been done in the past with π-A isotherms, BAM and GIXD [6]. She went further and studied a system with long alkyl chains and a soluble anion, such as $[C_{18}mim]^+[Cl]^-$, concluding that this system does not display a structured layer at the air-water interface.

The results were in line with experimental π-A isotherms obtained by researchers from Institut des NanoSciences de Paris, IST and Synchrotron SOLEIL, represented in Figure 1. The results show that the IL of $[C_{18}mim]^+$ $[Cl]^-$ does not display an organized structure, therefore not forming a Langmuir Monolayer.

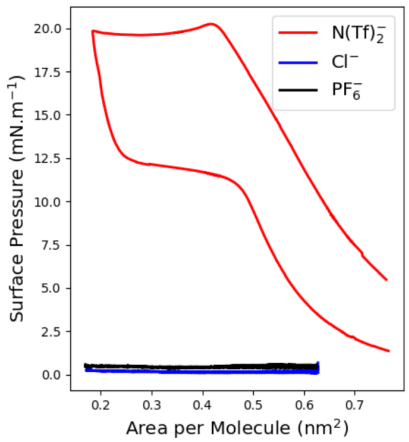

Figure 1: π-A isotherms for the ionic liquids $[C_{18}mim]^+[NTf2]$, $[C_{18}mim]^+[Cl]^-$, and $[C_{18}mim]^+[PF_6]$ first compression-expansion cycle.

From Figure 1 we can conclude that the $[C_{18}mim]^+[Cl]^-$ at the air-water interface does not behave like a Langmuir Film. Therefore, in this situation we have a Gibbs Monolayer, which is expectable since the IL is soluble in water.

It is important to mention, however, that the isotherms on Figure 1 are respective to the first compression and expansion cycle. In subsequent experiments, the research group observed an interesting behavior of $[C_{18}mim]^+[Cl]^-$ at the air-water interface. In Figure 2 subsequent compression-expansion cycles are represented. Filipe's research group noted that the isotherm started displaying a pressure increase that becomes bigger every 12 hours.

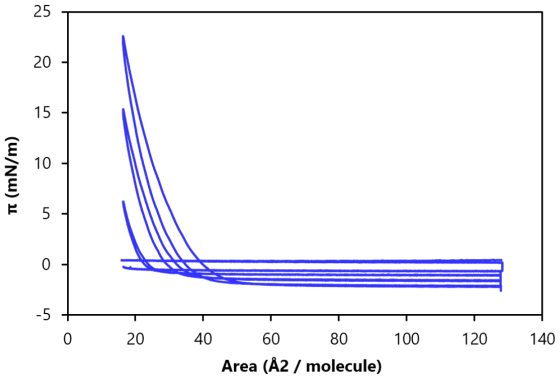

Figure 2: Langmuir Isotherms for continuous compression-expansion cycles for $[C_{18}mim]^+[Cl]^-$ at the surface of pure water.

An even more interesting behavior is observed in the case of $[C_{18}mim]^+[Cl]^-$ at the air-salted water interface, represented in Figures 3. The IL was placed in the interface at different $NaCl$ concentrations and a compression-expansion cycle was performed to obtain the π-A isotherm. The isotherm developed with the increase in salt concentration and, at the concentration of 0.5 M ($NaCl$), the $[C_{18}mim]^+[Cl]^-$ developed an isotherm very similar to the one observed with $[C_{18}mim]^+[NTf2]$, a IL which Colaço showed forms a trilayer at the surface of pure water. The isotherm profile obtained in salted water is stable after multiple compression-expansion cycles. These results are not yet published.

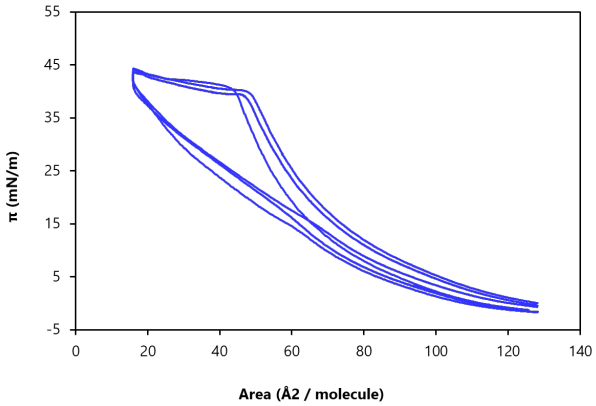

Figure 3: Langmuir Isotherms for continuous compression-expansion cycles for $[C_{18}mim]^+[Cl]^-$ at the surface of water with 0.5 M of $NaCl$.

2. Methodology

The basis for the work developed rests upon MD simulations of the $[C_{18}mim]^+$ Cl$^-$ IL at the air-water interface, and it was performed using the GROMACS 5.0.7 software package [7].

The force field used was the CL&P, developed by Canongia *et al* and optimized for the molecular modeling of ionic liquids of the dialkylimida-

zolium cation family. This force field was based on the OPLS-AA (optimized potentials for liquid simulations) and AMBER94 all-atom force fields, both of which have been widely used in the past for simulation of organic liquids and other compounds. [8, 9, 10]

With regards to the water molecules, the extended simple point charge model - SPC/E - was used [11, 12].

Each system was created in a step-by-step approach, starting with the formation of the layer of water by equilibrating the boxes with water molecules in a NPT ensemble, at constant pressure of 1 atm and temperature of 298.15 K, for 10 nanoseconds. The dimensions of the water boxes and subsequent number of water molecules in them varied for various simulations, according to the area per molecule and water layer thickness desired.

The next step is to extend the simulation box in the z-axis, originating an two air-water interfaces, in one of which the IL can be placed. Once again, the number of ionic pairs of IL added at this interface depends on the area per molecule desired. An example of initial configuration can be verified in Figure 4.

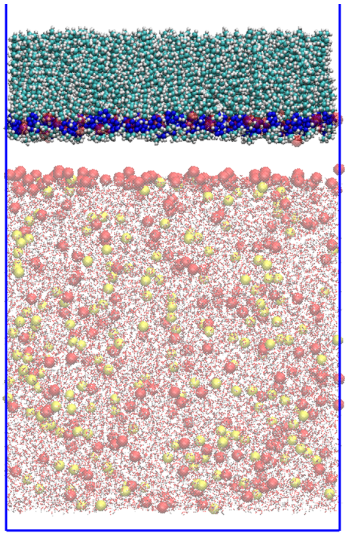

Figure 4: Initial configuration of a simulation box. Cyan/white licorice - $[C_{18}mim]^+$; blue licorice - imidazolium ring; red points - water; red spheres - chloride anions; yellow spheres - sodium cations.

The initial boxes were subject to an initial step for energy minimization, by undergoing through 25000 simulation steps with steepest descent algorithm. After that, a temperature ramp-up was applied to the IL molecules, from 50 K to 298 K, with the temperature elevation taking up to 0.5 ns. This gradual temperature elevation on the IL molecules is applied to avoid that these molecules develop a trajectory away from the water interface.

The production phase of the simulations was performed at 298.15 K, recurring to a Nosé-Hoover thermostat with time constants of 0.5 ps. For the Van der Waals and electrostatic interactions, a 1.6 nm cut-off was employed. For distances beyond the cut-off, long range electrostatic and Lennard-Jones interactions were calculated with the PME method. The time step employed was 2 fs.

The compression of a simulation box in the *xy*-plane was also studied. For the compression, a semi-isotropic pressure coupling was used and the compressibility of the medium was modified so as that the area of the surface halved every 2 ns, at minimum.

A quick analysis on the initial simulations led to the conclusion that the organization of the $[C_{18}mim]^+$ cations on the surface of water could use further tools in its categorization, apart from the ones available in GROMACS.

For instance, the alignment of the parallelism between the alkyl chains of the cations and the evolution of this alignment over time could help us further understand the driving force of the structures displayed and even help us define if the system is stabilized or not.

With this in mind, two Python scripts were developed, one to analyze the parallelism between alkyl chains and another one to analyze how ”vertical” the alkyl chains were.

3. $[C_{18}mim]^+$ $[Cl]^-$ at the air-water interface

Starting with the simulation of water boxes with 5, 10, 20 and 40 IP of IL deposited at the surface, with corresponding areas per molecule of 9.2, 4.6, 2.3 and 1.8 nm^2/molecule. Representative snapshots for these areas per molecule in Figure 5 suggest that the cations prefer to aggregate at the surface of the water. The system does not display isolated cations, suggesting that no gaseous phase is stable at this area per molecule. The cations tend to partially submerge in the water and the chloride anions tend solubilize.

These behaviors are explained by the properties of the system. The long alkyl chain of the $[C_{18}mim]^+$ cation favors the aggregation with other cations, in an attempt to minimize the interactions with the water surface. On the other hand, the chloride anions are hydrophilic and are solubilized in the water being observed at considerable distances from the surface. The partial submersion of the imidazolium is a consequence of it's hydrophilicity and the solubilization of the chloride anions. The partial submersion of the $[C_{18}mim]^+$ promotes the contact of the alkyl chains with the water, which contributes further to the aggregation of the cations.

The alkyl chains also tend to organize parallel

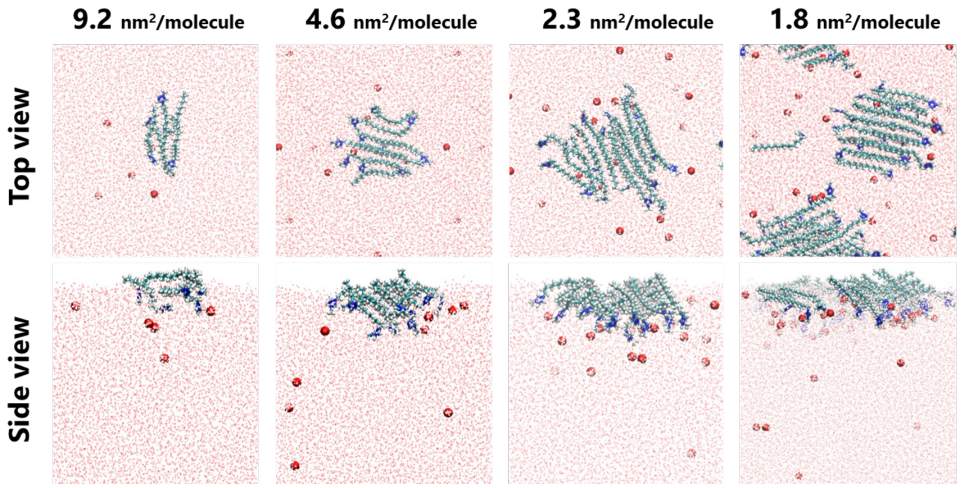

Figure 5: Top and side views of representative snapshots for simulation boxes at different areas per molecule.

in relation to each other. The reason for this alignment might be related to this organization maximizing the interaction between the chains, thus minimizing the interactions with the water surface. In Figure 6 it is possible to note that at the near-range, the alkyl chains tend to be anti-parallel[1]. The anti-parallel arrangement is favored by the repulsive interaction between the imidazolium heads, particularly important given the degree of separation of the chloride anions from the charged group of the cation. Furthermore, in Figure 7 it is possible to note that the system evolved in the way of favoring parallelism.

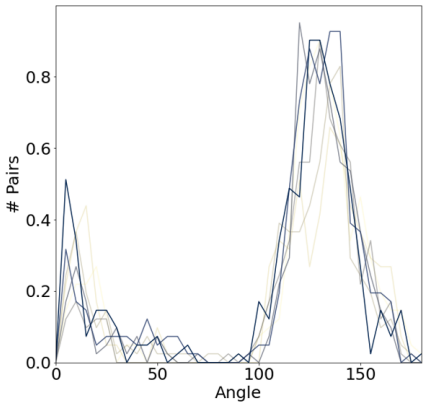

Figure 6: Distribution of angles between aklyl chains for a 0.5 nm cut-off. The graph represents the relation of the angle between alkyl chains and the number of pairs of cations that have each each angle. The lines result of an average over 2 ns of simulation and their represents the evolution over time of the system, light yellow being the more initial (around 11 ns) and dark blue being the end of the simulation (25 ns).

It is important to note that the force field used, CL&P, models the alkyl chains with extra rigidity, which might influence the organization of the chains, favoring the packing observed in the simulation results. [13, 14]

[1]The angle measurement between alkyl chains is made on a 3D level, therefore, since the cations are slightly submerged, an anti-parallel situation will be more approximated to a 140 º angle, rather than a 180 º, due to the inclination of the alkyl chains promoted by the submersion.

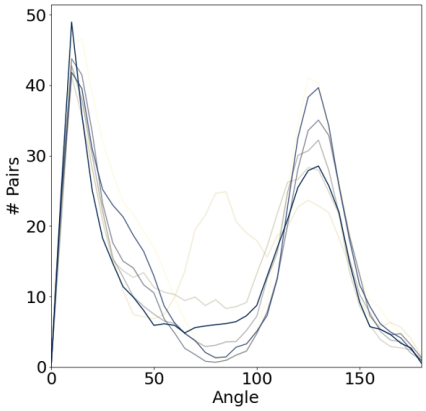

Figure 7: Distribution of angles between aklyl chains for a 4.25 nm cut-off.

It is also interesting to note that the visualizations of the parallelism and verticality analysis can help to understand if the simulation is still evolving or is reaching an equilibrium state. This is particularly important since 1-alkyl-3-methylimidazolium ILs are usually very viscous, despite having low melting points. This results in a very slow dynamics evolution of the simulated system, with the molecules moving at a very low rate, which poses as a problem regarding the MD simulation, that will require much more simulation time to reach equilibrium. Therefore, achieving a complete equilibrium state would take too much time, which is not possible according to the time available for the conclusion of this work [15].

The density profile of the simulation box, as in Figure 8, evidenciates the dissolution of a considerable number of $[Cl]^-$ in the water subphase. The chloride anions, despite being partially solubilized, maintain a certain proximity to the charged imida-

zolium ring because of the Coulombic attraction forces.

The cation's imidazolium ring, represented by the CR atom, is mainly submerged in water and the tail of the alkyl chain, represented by the atom CT, is mainly above water surface. The charged imidazolium head is hydrophilic and, therefore, is easily solubilized by the water. On the other hand, the alkyl chain is hydrophobic and favors the minimization of contact with water by staying at the surface in contact with the other alkyl chains and the vapor phase.

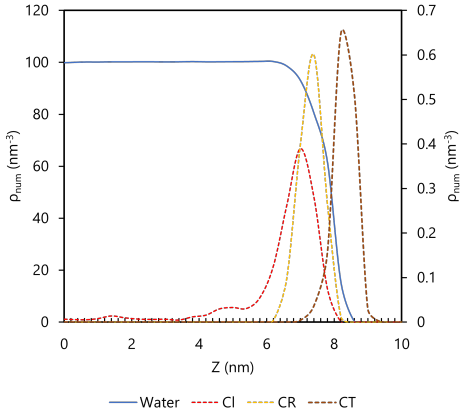

Figure 8: Number density profile for the simulation box with 20 000 waters and 40 IP of $[C_{18}mim]^+$ $[Cl]^-$ at a area per molecule of 1.8 nm^2/molecule. Density obtained for the simulation interval of 23 until 25 ns. Full lines for the main axis and dotted lines for the secondary axis.

With 20 000 water molecules and 100 IP deposited at the surface, the area per molecule becomes 0.725 nm^2/molecule. In Figure 9 it is noted that the aggregates maintains an high degree of organization.

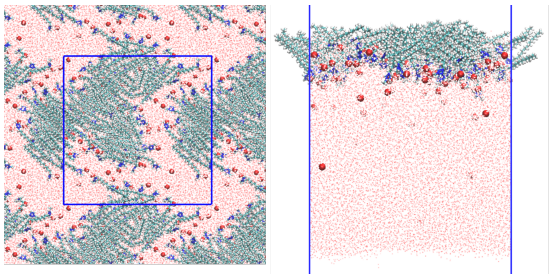

Figure 9: Snapshots of the simulation box with 20 000 water molecules and 100 ionic pair of $[C_{18}mim]^+$ $[Cl]^-$. (a) and (b) are top views of the simulation box at around 25 ns of simulation and (c) is a side view of the box at approximately the same time.

The density profile Figure 10 shows a similar structure to what was previously seen at a higher area per molecule. It is also possible to note that profile of the CR atom has a particular curvature, which might be related to the surface's structure.

At the area per molecule of 0.36 nm^2/molecule, on Figure 11, the $[C_{18}mim]^+$ cations agglomerate

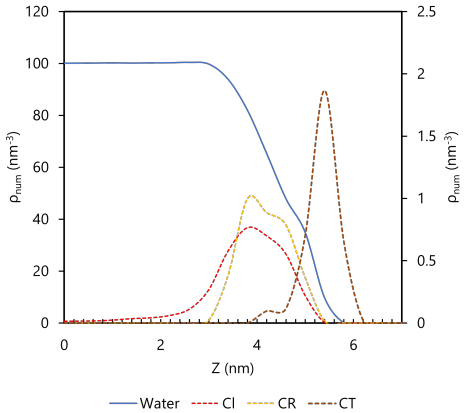

Figure 10: Number density profile for the simulation box with 20 000 waters and 100 IP of $[C_{18}mim]^+$ $[Cl]^-$ at a area per molecule of 0.725 nm^2/molecule. Density obtained for the simulation interval of 23 until 25 ns. Full lines for the main axis and dotted lines for the secondary axis.

as much as possible, leaving the charged imidazolium ring to the outside of the agglomerate. Free water is scarce, with the surface being significantly occupied by a fully formed monolayer. The evolution of the monolayer organization towards an elongated form on the *xy* axis suggests a structure similar to hemispherical cylinders. In this organization the aggregates are separated by free water zones where the concentration of chloride is higher, as can be seen on the density profile in Figure 13.

The side view of the simulation box also indicates structures resembling hemispherical cylinders. This evolution suggests that, at lower areas per molecule, these structures will converge, forming micelles at the bulk of the water.

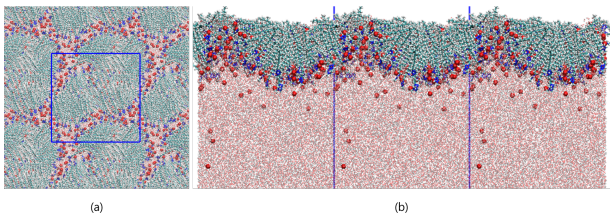

Figure 11: Snapshots of the simulation box with 20 000 water molecules and 200 ionic pair of $[C_{18}mim]^+$ $[Cl]^-$, at a area per molecule of 0.36 nm^2/molecule. (a) and (b) are top views of the simulation box at around 48 ns of simulation and (c) is a side view of the box at approximately the same time.

In Figure 12 it is possible to see a direct comparison of the angle with relation to the surface distribution for the different areas per molecule, noting the evolution towards more verticality when the surface is more compact.

Regarding the density profile in Figure 13, the first observation is regarding the curvature of the profile of the species near the surface, which is related to the structure of the surface aggregates and confirms past observations on Figure 10. Apart from that, the range of CR's profile increases from

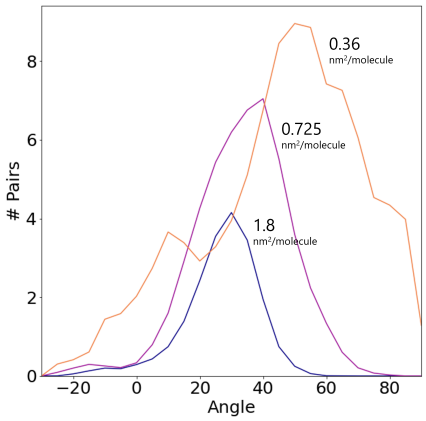

Figure 12: Comparison of the final distribution of angles obtained for the simulation of different areas per molecule.

2.4 nm at 0.725 nm^2/molecule to 6.6 nm at 0.36 nm^2/molecule.

One last observation is related to the dispersion of the chloride anions, which are much less dispersed and more concentrated near the imidazolium ring. In fact, comparing Figures 8, 10 and 13 we can see that the density profile of the chloride anions is more similar to the profile of the CR atom at increasingly lower areas per molecule. This suggests that the $[Cl]^-$ is closer to the imidazolium heads for lower areas per molecule, less dissolved in the water subphase.

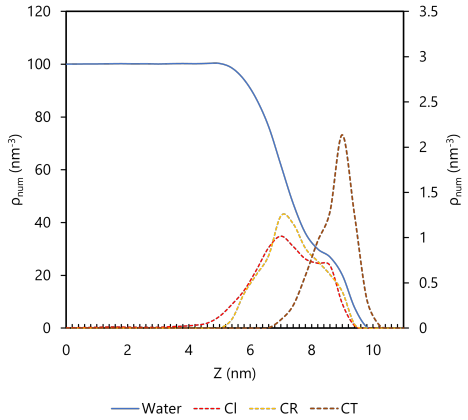

Figure 13: Number density profile for the simulation box with 20 000 waters and 200 IP of $[C_{18}mim]^+$ $[Cl]^-$ at a area per molecule of 0.36 nm^2/molecule. Density obtained for the simulation interval of 46 until 48 ns. Full lines for the main axis and dotted lines for the secondary axis.

The formation of micelles by systems of $[C_nmim]^+[Cl]^-$ has been experimentally verified in the past, with the CMC being obtained by Jungnickel *et al*. The CMC decreased considerably with the increase in size of the alkyl chain, being approximately equal to 0.43 mM for n=18 [16].

The classical idea for the formation of micelles is that these are formed upon compression of a fully formed monolayer. Therefore, the goal was now to observe what would happen if at even lower areas per molecule, with hypothesis that it would lead to the formation of micelles at the water's bulk.

For this reason a larger simulation box was built, which would allow to better understand the mechanism of formation of micelles upon compression. The simulation box consisted of 40 000 waters and 500 pairs of IL $[C_{18}mim]^+$ $[Cl]^-$. The water molecules were extended to maximize the surface area, which was 0.8 nm^2/molecule at the beginning of the simulation. The simulation box was stabilized at this area per molecule for 10 ns in an NVT ensemble and after was subjected to compression. For the compression, an NPT ensemble with semi-isotropic compression was employed, with the compressibility factors being altered so as that the surface area halved every 2 ns.

The first step was to compress the simulation box to a area per molecule of 0.36 nm^2/molecule. At this density, the system was stabilized by a 10 ns simulation in a NVT ensemble before being further compressed until the area per molecule of 0.24 nm^2/molecule. In Figure 14 it is clear the formation of micelles, with some molecules submerging from the surface into the water, upon compression.

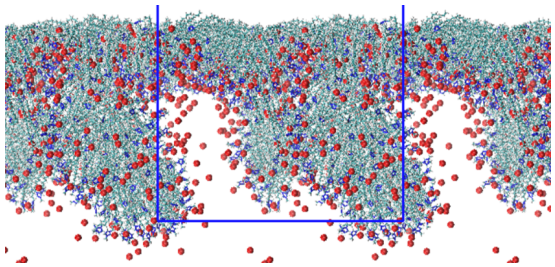

Figure 14: Side view of the system with 500 IP of IL at the surface of 40 000 water molecules, after compression to area per molecule of 0.24 nm^2/molecule and stabilization for 20 ns.

Despite the snapshots in Figure 14 indicating that the formation of micelles is imminent, the dynamic evolution of the system was very slow. Therefore, the simulation box was submitted to an annealing process, in an attempt to accelerate the possible formation of micelles. The system's temperature was increased to 373.15 K, staying at that temperature for 8 ns, before decreasing back to 298.15 K.[2]

This annealing procedure led to the formation of 2 aggregates that separated themselves from the surface of water and submerged. The aggregation numbers for these aggregates were 115 and 156, leaving 229 ionic pairs at the surface. As can be seen in Figure 15, the micelles formed are not as spherical as the one formed previously.

With only 229 remaining at the surface, the area per molecule is approximately 0.51 nm^2/molecule.

[2]Each temperature increase/decrease was done with a linear variation over time, with the total duration of 1 ns.

Previous simulations showed that the surface was stable at a density as low as 0.36 nm^2/molecule and extrapolations of experimental results predict an aggregation number of 115 for this IL. One could argue that the simulation is not yet stabilized and that, if given more time, some molecules would migrate from the larger micelle to the surface.

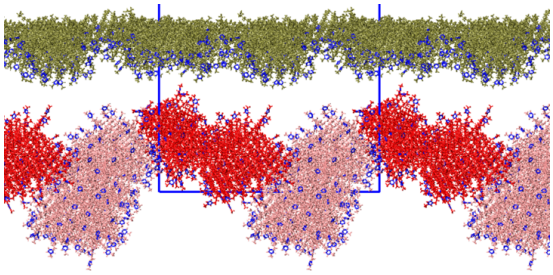

Figure 15: Side views for the simulation box compressed to 0.24 nm^2/molecule, after annealing for 8 ns at 373.15 K, without representation of waters. Surface layer represented with dark yellow, aggregate with 156 molecules represented in pink, aggregate with 115 molecules represented in red and imidazolium rings represented in blue.

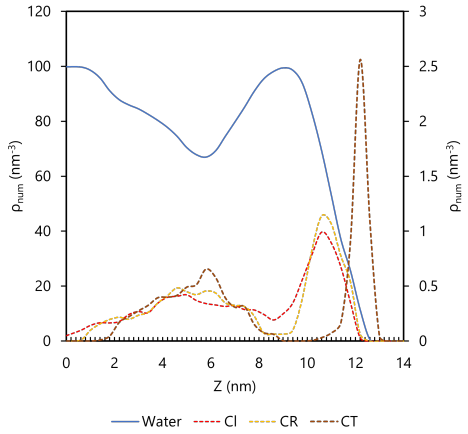

Figure 16: Number density profile for the simulation box with 40 000 waters and 500 IP of $[C_{18}mim]^+$ $[Cl]^-$ at a area per molecule of 0.24 nm^2/molecule, after annealing at 373.15 K for 8 ns. Full lines for the main axis and dotted lines for the secondary axis.

It is very clear at this point that simulations are able to predict that the IL of $[C_{18}mim]^+$ $[Cl]^-$ leads to the formation of micelles, with 3 of them being formed in the work so far, which is in agreement with experimental data. The aggregation numbers of such micelles were 95, 115 and 156, leading to an average aggregation number of 122, very close to the estimation by Colaço of 115.

4. $[C_{18}mim]^+$ $[Cl]^-$ at the air-salted water interface

To elucidate about the reasons behind the behavior of $[C_{18}mim]^+[Cl]^-$ at the air-salted water interface, the systems simulated with pure water were simulated again, but this time in water with 0.5 M of $NaCl$. The goal is to compare the results in both situations and use that information to help suggest possible explanations for the observable differences in behavior. Only systems at a lower area per molecule were simulated, since there are limited computational resources and at lower areas per molecule the surface is more compact, which might reveal more important details about the organization. Therefore, the higher area per molecule simulated in the air-salted water interface was 0.725 nm^2/molecule.

Starting by analyzing a simulation at 0.725 nm^2/molecule, in a box of 30 000 water molecules and 271 $NaCl$ ions, 250 $[C_{18}mim]^+[Cl]^-$ were deposited normal to the surface, for the initial configuration. A 60 ns simulation in a NVT ensemble was performed. Figure 17 shows the final configuration.

The IL organized at the surface in two independent aggregates, with 75 and 175 cations composing each aggregate. While the simulation in pure water at the same density was not as big as this one in terms of number of molecules, the results suggest that in both cases the cations have the tendency to aggregate at the surface.

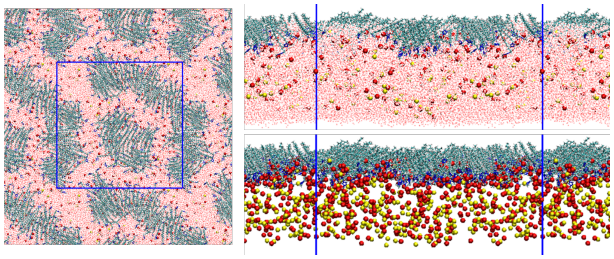

Figure 17: Visualization of a system with 30 000 waters and 271 pairs of $[Na]^+[Cl]^-$, with 250 pairs of $[C_{18}mim]^+$ $[Cl]^-$ at the surface, corresponding to a area per molecule of 0.725 nm^2/molecule, after 60 ns of simulation in a NVT ensemble. On the left, the top view; on the right top and bottom, the side view with and without the representation of the water molecules, respectively.

With the regards to how the cations organize themselves, there are slight differences between the simulations with and without water. Starting with the density profile in Figure 18, the imidazolium rings have a much closer presence of chloride anions that, due to the chloride concentration in water itself, have a higher tendency to stay near the charged imidazolium ring.

The density profile suggests that the salt in solution has a slight effect on the organization of the different species at the surface. Regarding the surface water layer thickness, it is approximately 0.2 nm smaller in salted water when compared to pure water and equal to 2.8 nm, and it is worth noting that the concentration of the CR atom, representing the imidazolium ring, is slightly more concentrated near the surface in salted water than in pure water. The same happens for the tail of the alkyl chain, represented by the CT atom.

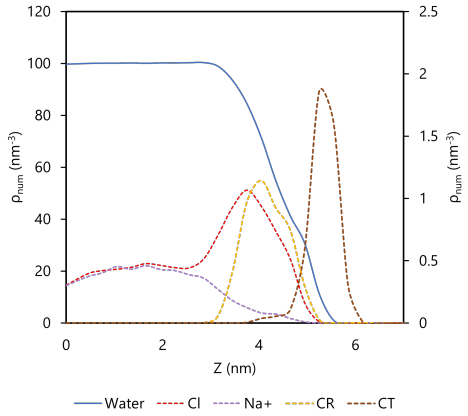

Figure 18: Numerical density profile for the simulation with 30 000 waters and 271 pairs of $[Na]^+[Cl]^-$, with 250 pairs of $[C_{18}mim]^+$ $[Cl]^-$ at the surface, corresponding to a area per molecule of 0.725 nm^2/molecule. Left axis for water profile and right axis for remaining profiles. CR is the one of the carbons of the imidazolium ring and CT is the terminal carbon of the alkyl chain.

This might be a slight indicator of a salting-out effect, that could be an explanation for the behavior observed on the Langmuir Trough. The $NaCl$ in solution helps to stabilize the surface layer, with the chloride anions staying near the $[C_{18}mim]^+$ and providing some sort of support for the cations. This support provides the necessary stability for the structure to start exhibiting a isotherm resembling a Langmuir Film, instead of a Gibbs Film.

Going for lower areas per molecule, where the system is even more compacted at the surface, a system with 200 ionic pairs at the surface of box with 20 000 water molecules and 185 pairs of $[Na]^+[Cl]^-$ (0.5 M of NaCl) was simulated, corresponding to a area per molecule of 0.36 nm^2/molecule. Figure 19 shows final configuration..

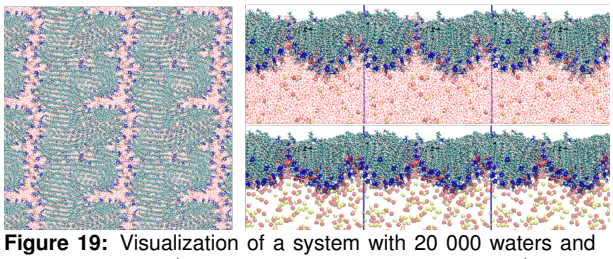

Figure 19: Visualization of a system with 20 000 waters and 185 pairs of $[Na]^+[Cl]^-$, with 200 pairs of $[C_{18}mim]^+$ $[Cl]^-$ at the surface, corresponding to a area per molecule of 0.36 nm^2/molecule, after 80 ns of simulation in a NVT ensemble. On the left, the top view; on the right top and bottom, the side view with and without the representation of the water molecules, respectively.

The top view suggests that when an electrolyte, such as NaCl, is present in water, the ionic liquid at the surface tends to form a continuous aggregate, as opposed to what happened in simulations with the same area per molecule but without salt, as can be seen in Figures 11 and 14 (c). This surface arrangement can be a decisive factor to explain the stability of the surface leading to the formation of an isotherm in the Langmuir Trough.

The side view of the surface displays hemispherical cylinder arrangements, which are smaller than the ones observed without salt, in Figure 11. While in pure water only one arrangement was observed, in this situation two arrangements are present.

The density profile in Figure 20 supports further the idea of a salting-out effect of the cations in the presence of an electrolyte in water. The water layer thickness at the surface with salt is 4.4 nm, as opposed to 4.8 in pure water.

In addition, the cation's tails (represented by the dotted CT curve) are much more concentrated at the surface, with the peak of the density curve being around 3.0 nm^{-3} (vs 2.1 nm^{-3} in pure water), and the thickness also being smaller.

The chlorides are even more close to the cations imidazolium (compared to Figure 18, in a system with salted water at a higher area per molecule). This can suggest that the chlorides are providing a higher support for the cations at the surface, thus stabilizing them.

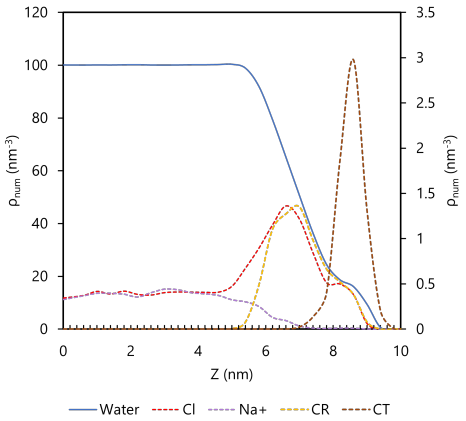

Figure 20: Number density profile for the simulation box with 20 000 waters, 185 pairs of $[Na]^+[Cl]^-$ (0.5 M) and 200 IP of $[C_{18}mim]^+$ $[Cl]^-$ at a area per molecule of 0.36 nm^2/molecule. Full lines for the main axis and dotted lines for the secondary axis.

Figure 21 shows that the system in salted water is more vertical than the one in pure water, with less alkyl chains making an angle to the surface of water of around 0 °, and more making an angle of around 90 °. This extra perpendicularity to the water's surface suggest an approximation to the organization of $[C_{18}mim]^+[NTf_2]^-$ at the surface of water, which leads to Langmuir layers.

The final simulation consisted of 500 IP deposited at the surface of 40 000 water molecules with a $[Na]^+[Cl]^-$ concentration of 0.5 M, for a area per molecule of 0.8 nm^2/molecule. After running the simulation in an NVT ensemble for 10

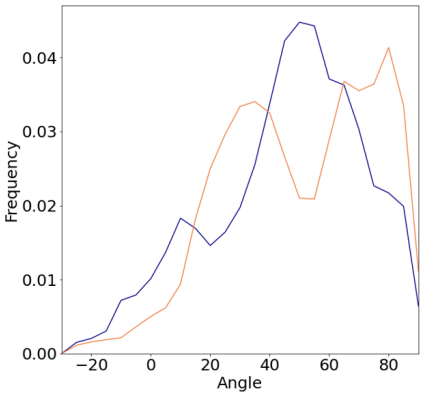

Figure 21: Comparison of verticality for simulations at a area per molecule of 0.36 nm^2/molecule: Blue - with pure water; Orange - with salted water;

ns, the simulation box was compressed to 0.36 nm^2/molecule. At this area per molecule, the simulation ran for 20 ns in an NVT ensemble, after which it was compressed to the area per molecule of 0.24 nm^2/molecule. Snapshots with the evolution of the system are available in Figure 22.

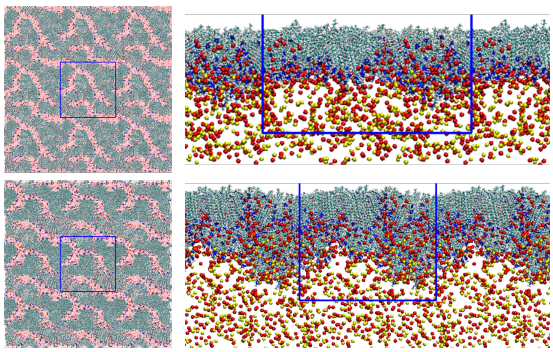

Figure 22: Top and side view of the evolution over time of the system with 40 000 waters with a $[Na]^+[Cl]^-$ concentration of 0.5 M and 500 pairs of $[C_{18}mim]^+$ $[Cl]^-$ at the surface. From top to bottom: 0.36 nm^2/molecule, after compression and 20 ns in a NVT ensemble; 0.24 nm^2/molecule, after compression. The waters were omitted to facilitate the observation of the formation of the micelle.

Figure 22 suggests, once again, that at the area per molecule of 0.36 nm^2/molecule, the surface's cations have a tendency to agglomerate continuously, taking into consideration the PBC. The simulation also suggests that even in salted water there is the formation of micelles, with some cations from the surface submerging into the bulk at the area per molecule of 0.24 nm^2/molecule.

5. Conclusions

The objective of this work consisted on helping understand the behavior of the ionic liquid in both in pure and salted water.

The simulation in pure water varied in size and areas per molecule. The higher areas per molecule simulated were of 9.2 nm^2/molecule, with 5 ionic pairs deposited at the surface of 10 000 water molecules and the lower being 0.24 nm^2/molecule, with 500 ionic pairs deposited at the surface of 40 000 water molecules.

The results suggested that even at high areas per molecule, the cations at the surface tend to aggregate. The surface aggregates are very organized, with the alkyl chains parallel to each other. This parallel arrangement tends to be seen throughout all the simulations, suggesting an attempt to minimize energy by maximizing the interactions between the hydrophobic chains of the cations and minimizing the contact with water.

In fact the molecules are not only parallel, but tend to be in an anti-parallel arrangement, displaying a sort of double interdigitated layer. This arrangement is crucial given the fact it was observed that in these systems a considerable number of chloride anions tend to dissolve in water, stepping further away from the cation's charged ring. This causes the imidazolium heads to have high repulsive forces between them, thus organizing themselves in an anti-parallel arrangement to minimize such forces. In a brief comparison with systems of $[C_{18}mim]^+$ $[NTf_2]^-$ the same does not happen, since the anions are highly hydrophobic and do not dissolve, organizing in a chessboard arrangement with the imidazolium heads.

The results also show that the solubility of the chloride anions might cause the cations to partially submerge more in comparison to the system with $[NTf_2]^-$, as can be seen from the differences in the water layer surface thickness at approximately 0.36 nm^2/molecule (1.5 nm for $[C_{18}mim]^+$ $[NTf_2]^-$ and 4.8 nm for $[C_{18}mim]^+$ $[Cl]^-$).

At lower areas per molecule, the cations at the surface are more compacted. At 0.36 nm^2/molecule, the simulation results suggest the formation of hemispherical cylinders at the surface of water. Further compression of the surface to 0.24 nm^2/molecule showed the formation of micelles in the water's bulk. The aggregation numbers obtained for different micelles in pure water were 95, 115 and 156, for an average of 122, very close to the estimation of 115 by Colaço [6].

The analysis on the structure of the surface cations concluded that the alkyl chains are more vertical for lower areas per molecule, with the majority of the alkyl chains making an angle of 50 º with the surface at the areas per molecule of 0.36 nm^2/molecule.

The density profile analysis showed that the water's surface layer thickness was inferior and concentration of alkyl chains above the water surface was higher. It also suggested a smaller dislocation of the chloride anions, which might be related to the concentration of $NaCl$ already present in the bulk of the water. The verticality analysis

also showed a tendency for the alkyl chains to be more perpendicular to the water's surface when an eletrolyte is present.

Visual analysis of the simulations with salted water also showed what might be a more stable organization. At 0.36 nm^2/molecule, the cations on the surface aggregate continuously, taking into account the PBC. Along side that, the hemispherical cylinders formed are smaller. While in simulation in pure water, all the 200 cations aggregated and formed 1 hemispherical cylinder, in salted water the 200 cations formed 2. This arrangement might prove to be more stable, leading to the results observed in the Langmuir Trough.

The simulations predict that there is still the formation of micelles that submerge to the bulk of the salted water, in accordance to experimental data.

It is important to mention that the results obtained so far do not help us fully explain the experimental data obtained in the Langmuir Trough. The *plateau* observed in Figure 3 for $[C_{18}mim]^+[Cl]^-$ at the surface of water with 0.5 M of $NaCl$ is similar to the one obtained for $[C_{18}mim]^+[NTf_2]^-$ in Figure 1, which is known to correspond to the formation of a trilayer structure. This structure formation was also verified with MD simulations [5].

In the case of $[C_{18}mim]^+[Cl]^-$, however, the simulation data does not predict the formation of a trilayer structure. Instead, at molecular areas corresponding to the plateau in Figure 3, the simulations predict the formation of micelles. This micelle formation was expected, due to the experimental data that provides CMC values in salted water and the simulations' results also show that. The question that remains unanswered is the effect that having $NaCl$ dissolved in water causes to the stability of the surface.

One hypothesis could suggest that the results observed in pure water, with the surface pressure increasing over time, are a result of a surface organization with very slow kinetics, which could be explained due to the high viscosity of the system. In that case, the salt in water would have a catalytic effect over the kinetics of organization. Another hypothesis is that the added proximity of the chloride anions to the imidazolium heads in the case of salted water helps stabilize the system. Obviously, both hypothesis could be wrong and many more can be drawn.

References

[1] P. Wasserscheid, "Volatile times for ionic liquids," *Nature*, vol. 439, pp. 797–797, Feb 2006.

[2] A. J. Greer, J. Jacquemin, and C. Hardacre, "Industrial applications of ionic liquids," *Molecules*, vol. 25, no. 21, 2020.

[3] H. Ibrahim, *Study of (C20mim) + (NTf2) - ionic liquid Langmuir films mixed with graphene oxide sheets or deposited on aqueous gold ion subphases and irradiated by grazing incidence X-rays*. Theses, Sorbonne Université, Dec. 2020.

[4] V. Kaganer, H. Möhwald, and P. Dutta, "Structure and phase transitions in langmuir monolayers," *Reviews of Modern Physics*, vol. 71, pp. 779–819, Apr. 1999.

[5] E. J. M. Filipe, P. Morgado, M. Teixeira, K. Shimizu, N. Bonatout, M. Goldmann, and J. N. C. Lopes, "Crystalline-like structures and multilayering in langmuir films of ionic liquids at the air–water interface," *Chemical Communications*, vol. 52, no. 32, pp. 5585–5588, 2016.

[6] B. Colaço, "Interfaces of ionic liquids," *Master thesis, Instituto Superior Técnico, Lisboa*, 2020.

[7] D. Van Der Spoel, E. Lindahl, B. Hess, G. Groenhof, A. E. Mark, and H. J. C. Berendsen, "Gromacs: Fast, flexible, and free," *Journal of Computational Chemistry*, vol. 26, no. 16, pp. 1701–1718, 2005.

[8] J. N. Canongia Lopes, J. Deschamps, and A. A. H. Pádua, "Modeling ionic liquids using a systematic all-atom force field," *The Journal of Physical Chemistry B*, vol. 108, pp. 2038–2047, Feb 2004.

[9] W. L. Jorgensen and J. Tirado-Rives, "Monte carlo vs molecular dynamics for conformational sampling," *The Journal of Physical Chemistry*, vol. 100, pp. 14508–14513, Jan 1996.

[10] G. Kaminski and W. L. Jorgensen, "Performance of the amber94, mmff94, and opls-aa force fields for modeling organic liquids," *The Journal of Physical Chemistry*, vol. 100, pp. 18010–18013, Jan 1996.

[11] H. J. C. Berendsen, J. R. Grigera, and T. P. Straatsma, "The missing term in effective pair potentials," *The Journal of Physical Chemistry*, vol. 91, pp. 6269–6271, Nov. 1987.

[12] V. Vinš, D. Celný, B. Planková, T. Němec, M. Duška, and J. Hrubý, "Molecular simulations of the vapor–liquid phase interfaces of pure water modeled with the SPC/e and the TIP4p/2005 molecular models," *EPJ Web of Conferences*, vol. 114, p. 02136, 2016.

[13] M. L. P. Price, D. Ostrovsky, and W. L. Jorgensen, "Gas-phase and liquid-state properties of esters, nitriles, and nitro compounds with the OPLS-AA force field," *Journal of Computational Chemistry*, vol. 22, no. 13, pp. 1340–1352, 2001.

[14] S. W. I. Siu, K. Pluhackova, and R. A. Böckmann, "Optimization of the OPLS-AA force field for long hydrocarbons," *Journal of Chemical Theory and Computation*, vol. 8, pp. 1459–1470, Mar. 2012.

[15] K. R. Seddon, A. Stark, and M.-J. Torres, "Viscosity and density of 1-alkyl-3-methylimidazolium ionic liquids," in *ACS Symposium Series*, pp. 34–49, American Chemical Society, May 2002.

[16] C. Jungnickel, J. Łuczak, J. Ranke, J. F. Fernández, A. Müller, and J. Thöming, "Micelle formation of imidazolium ionic liquids in aqueous solution," *Colloids and Surfaces A: Physicochemical and Engineering Aspects*, vol. 316, no. 1, pp. 278–284, 2008.